SI Methods

Collection and analysis of fecal metagenomic data from public cognitive impairment-related cohorts and 5-FU-treated cohorts

To characterize alterations in gut microbiota-derived ammonia in human populations, we downloaded fecal metagenomic sequencing data from publicly available cohorts of patients with MCI [1]. In addition, to evaluate whether 5-FU exposure itself was associated with microbial urease or ammonia-producing potential, a paired public fecal metagenomic cohort before and after 5-FU treatment was included. This 5-FU cohort was derived from a previously published chemotherapy-related gut microbiome study, in which fecal samples were collected before treatment and after 5-FU exposure [2]. The data were analyzed following the workflow described in the section "Metagenomic sequencing and analysis of fecal samples"**.**

Recruitment and characterization of the independent clinical cohort

To examine gut microbiota-derived ammonia metabolism in an independent clinical cohort, healthy controls and patients diagnosed with MCI were recruited. Cognitive performance was assessed using the MMSE and MoCA. Demographic and clinical characteristics, including age, sex, diabetes, hypertension, coronary heart disease, and dyslipidemia, were recorded and compared between groups. Dietary information was collected based on the standardized meal records provided by the elderly care facility. All participants received meals from the same facility. The meals were generally vegetable-dominant and lightly seasoned, with animal protein provided as a supplementary component. Typical food items included staple foods, vegetables, animal-protein sources, soy products, and soups, as summarized in **Supplementary Figure 8A**. Because individual-level quantitative dietary intake was not available, dietary intake was not included as a formal covariate in the statistical model.

All participants provided written informed consent, and all patient information was anonymized before analysis. Exclusion criteria included the use of laxatives, probiotics, antidiarrheals, glucocorticoids, immunosuppressants, antitumor agents, or antibiotics before sample collection. The study was reviewed and approved by the Institutional Review Board of the School of Basic Medical Science, Central South University (No. 2021-KT75).

Fecal sample collection and measurement of fecal ammonia and urease activity

Fresh fecal samples were collected using a standardized protocol to minimize pre-analytical variation in ammonia measurement. Because ammonia is unstable and its quantification can be affected by delayed processing, temperature, storage conditions, and repeated freeze-thaw cycles, sample handling was performed with reference to previously recommended pre-analytical principles for ammonia evaluation [3]. Participants were instructed to collect fecal samples into sterile airtight collection tubes. Samples were sealed immediately after collection, transported to the laboratory on ice within a fixed time window, and stored at -80 ℃ until analysis. During ammonia quantification, fecal samples were thawed only once, weighed, homogenized in pre-chilled extraction buffer, and centrifuged at 4 ℃ to obtain the supernatant. Fecal ammonia concentrations were measured promptly using the Ammonia Content Assay Kit (G0436W, Grace Biotechnology) according to the manufacturer's instructions. Fecal urease activity was measured using the Urease (UE)Activity

Assay Kit (BC4115, Solarbio, Beijing, China) according to the manufacturer's protocol.

Blood collection, plasma Aβ42 measurement, and APOE genotyping

Peripheral blood samples were collected from participants using EDTA anticoagulant tubes. After collection, blood samples were gently inverted several times to ensure adequate anticoagulation, temporarily kept on ice, and transported promptly for processing. Plasma separation was performed as soon as possible after blood collection to minimize pre-analytical variation. Samples were centrifuged at 4,000 rpm for 10 min at 4 ℃, and the plasma fraction was carefully collected, aliquoted into sterile tubes, and stored at -80 ℃ until analysis. Repeated freeze-thaw cycles were avoided.

Plasma Aβ42 levels were measured using a Human Aβ1-42(Amyloid Beta 1-42) ELISA Kit (E-EL-H0543, Elabscience) according to the manufacturer's instructions. Briefly, plasma samples and standards were added to antibody-coated plates, followed by incubation, washing, enzyme-conjugated detection, substrate reaction, and absorbance measurement. Aβ42 concentrations were calculated from the standard curve.

For APOE genotyping, genomic DNA was extracted from peripheral blood samples using a commercial genomic DNA extraction kit according to the manufacturer's protocol. The APOE region covering the two defining single-nucleotide polymorphisms, rs429358 and rs7412, was amplified by PCR using the following primers:

APOE-F, 5'-AGGGCGCTGATGGACGAGAC-3'
APOE-R, 5'-GCTCACGGATGGCGCTGAGG-3'

PCR was performed using a commercial PCR master mix, with an initial denaturation at 98 ℃ for 2 min, followed by 35 cycles of 98 ℃ for 10 s, 56 ℃ for 10 s, and 72 ℃ for 10 s/kb, and a final extension at 72 ℃ for 5 min. PCR products were verified by agarose gel electrophoresis and then subjected to Sanger sequencing using an ABI 3730 sequencer. Sequencing chromatograms were inspected at rs429358 and rs7412, and APOE genotypes were assigned as ε2, ε3, or ε4 based on the combined nucleotide pattern at these two loci. APOE ε4 carrier frequency was defined as the proportion of individuals carrying at least one ε4 allele, and APOE ε4 allele frequency was defined as the proportion of ε4 alleles among all APOE alleles. Differences in ε4 carrier frequency and ε4 allele frequency between groups were assessed using Fisher's exact test.

Metagenomic sequencing and analysis of fecal samples

To assess alterations in functional genes within the gut microbiome, total genomic DNA was extracted using OMEGA Soil DNA Kit (Omega Bio-Tek). Sequencing libraries with an insert size of approximately 400 bp were constructed using the NEXTFLEX Rapid DNA-Seq Kit and sequenced on the Illumina HiSeq X-ten platform in paired-end mode (PE150) by Shanghai BIOZERON Biotechnology Co., Ltd. Raw sequencing reads were subjected to quality control using Fastp, Bowtie2, and Fastuniq, followed by de novo assembly into contigs with Megahit [4-7]. Taxonomic profiling was performed using Kraken2, and abundance estimates were refined and normalized with Bracken [8, 9]. Functional genes were predicted by Prodigal, redundancy removed by CD-HIT, coverage estimated with Salmon, and functional annotation performed with eggNOG-mapper [10-13]. KEGG pathways and urease-related differential genes were analyzed using the Mann-

Whitney U test with FDR correction. The bacterial host that contributes ure gene was identified by Kraken2.

Animals and housing conditions

Ten-week-old specific-pathogen-free (SPF) male Kunming mice were used for the 5-FU-induced MCI-like model, NH_4Cl treatment, and bacterial intervention experiments. Kunming mice were obtained from Hunan Sleek Jingda Laboratory Animal Co., Ltd. (Changsha, China). For AD-related genetic-model validation, 8-week-old male 5xFAD mice and age-matched male control mice were purchased from Shulaibao (Wuhan) Biotechnology Co., Ltd. (Wuhan, China). All animals were maintained under controlled environmental conditions, including a temperature of 25 ± 5 ℃, relative humidity of 60-70%, and a 12-h light/dark cycle. Mice had free access to water and standard laboratory chow throughout the experiment. All mice received the same chow diet to minimize dietary variation in nitrogen intake and ammonia production. The nutrient composition of the chow was as follows: crude protein >18%, crude fat >4%, crude fiber <5%, crude ash <8%, moisture <10%, calcium 1.0-1.8%, and phosphorus 0.6-1.2% (**Supplementary Figure 8B**). All procedures were conducted in accordance with the National Institutes of Health Guide for the Care and Use of Laboratory Animals and were approved by the Institutional Ethics Committee for Animal Procedures of Central South University (CSU-2024-0315).

Co-housing and urease-inhibition rescue experiment

To determine whether MCI-associated gut microbial alterations could transmit an ammonia-related cognitive phenotype, WT mice were co-housed with MCI mice in the same cage. Age-matched WT mice housed separately under the same conditions served as controls. During the co-housing period, fecal samples were collected to monitor changes in intestinal ammonia levels. Because co-housing transfers the entire gut microbial community rather than ammonia alone, an additional urease-inhibition rescue experiment was performed to evaluate whether the transmitted phenotype depended on bacterial urease-mediated ammonia production. Cohoused WT mice were treated with the bacterial urease inhibitor FFA (6 mg/kg, intraperitoneally), while cohoused control mice received vehicle treatment. After the co-housing period, cognitive performance was assessed using behavioral tests, including the Y-maze test, novel object recognition test, and Morris water maze test. Fecal ammonia levels were measured after treatment to determine whether FFA reduced intestinal ammonia accumulation in cohoused WT mice.

Assessment of cognitive and memory functions

To assess the degree of cognitive impairment, mice underwent Y-maze, novel object recognition, and Morris water maze tests. Detailed experimental procedures for each behavioral assay are described below.

Y-Maze test The Y-maze test exploits the innate preference of rodents for novelty to assess spontaneous exploratory behavior and short-term spatial working memory. The apparatus comprised three identical arms arranged symmetrically at 120° angles and connected at a central junction. At the start of each trial, mice were gently placed at the center of the maze facing a predefined orientation. Exploratory activity was recorded under standardized environmental conditions for 8 min. An arm entry was defined as the placement of all four limbs into an arm. The sequence of arm entries was documented, and a spontaneous alternation was defined as consecutive entries into three

different arms. The spontaneous alternation percentage was calculated using the following formula:

$$\text{Alternation rate (\%)} = [\text{Number of Alternations} / (\text{Total Arm Entries} - 2)] \times 100\%$$

The subtraction of two entries reflects the minimum number of arm visits required to generate the first possible alternation.

Novel Object Recognition test The NOR test was performed in an opaque open-field arena to evaluate recognition memory. Two identical objects (A1 and A2) and one novel object (B) were used. Day 1 (familiarization phase): Two identical objects (A1 and A2) were placed in adjacent corners of the arena. Mice were placed gently in the center of the arena with starting orientation counterbalanced to avoid directional bias. Experiments were conducted in a sound-isolated room with blackout curtains to minimize external disturbances. Exploratory behavior was recorded for 10 min, during which locomotor activity and object exploration time were quantified. Mice were then returned to their home cages. Day 2 (test phase): One of the familiar objects was replaced with the novel object (B), while object positions were otherwise unchanged. Mice were subjected to a second 10-min exploration session, and the time spent exploring the familiar and novel objects was recorded.

Morris Water Maze test Spatial learning and memory were assessed using the Morris water maze. The apparatus consisted of a circular pool (150 cm diameter, 50 cm height) filled with water maintained at 22-24 ℃. Titanium dioxide was added to make the water opaque. A circular escape platform was submerged 1 cm below the water surface in a fixed quadrant. Distal visual cues were placed around the pool to facilitate spatial navigation. The experiment included an acquisition phase (days 1-4) followed by a probe test (day 5). Acquisition phase: Mice underwent three trials per day, each lasting up to 60 s, with inter-trial intervals of at least 30 min. Starting locations were pseudo-randomized among the non-target quadrants. A trial was considered successful when the mouse remained on the platform for at least 3 s. Mice that failed to locate the platform within 60 s were guided to it and allowed to stay for 20 s. Escape latency was averaged across daily trials and used as the primary learning index. Probe test: On day 5, the platform was removed. Mice were released from the quadrant opposite the former platform location, and the number of crossings over the original platform position during a 60-s trial was recorded as an index of memory retention.

Isolation of urease-positive bacteria from MCI patient's feces

To isolate urease-positive bacteria, fecal samples collected from MCI patient were used. Fecal samples were resuspended in PBS and allowed to stand for 5 min to permit particulate matter to settle. The resulting supernatant was spread onto urea phenol red (UPR) agar plates. Colonies producing a visible red color change were selected as putative urease-positive isolates and purified through three successive rounds of streaking on fresh UPR agar. Pure isolates were taxonomically identified by amplification of the full-length 16S rRNA gene using universal primers, followed by Sanger sequencing. Sequence identity was determined using BLASTn searches against the NCBI RefSeq database. All confirmed isolates were preserved at -80 ℃ in glycerol stocks for subsequent experiments.

Construction and validation of recombinant *E. coli* BL21 expressing Lfus-urease

Recombinant Escherichia coli BL21 strains expressing Lfus urease were generated as described in our previous study [14]. In brief, the urease-encoding genes *ureA*, *ureB*, and *ureC* identified from the

whole-genome sequencing of *Lysinibacillus fusiformis* were heterologously expressed in Escherichia coli BL21 (DE3) (B528414, Sangon Biotech). The recombinant plasmids were transformed into E. coli BL21 (DE3). Expression of the three urease subunits was confirmed by Tris-Tricine SDS-PAGE. Protein bands of interest were subjected to in-gel tryptic digestion, followed by high-resolution liquid chromatography-mass spectrometry (LC-MS) analysis using an Orbitrap Astral mass spectrometer coupled to a Vanquish NEO system (BIORUN BIOSCIENCES) [14]. Recombinant Escherichia coli BL21 was cultured separately in 200 mL lysogeny broth (LB) at 37 ℃ with shaking at 200 rpm for 48 h to generate bacterial suspensions. Following antibiotic treatment, mice were administered 0.2 mL of the corresponding bacterial suspension by oral gavage.

P. fortuita intervention and FFA rescue in mice

Urease-positive bacterial strains, including *E. faecium*, *K. oxytoca*, and *P. fortuita*, were isolated from human fecal samples as described above. For in vivo bacterial intervention, mice were first treated with a 7-day antibiotic cocktail in drinking water to deplete the endogenous gut microbiota. The antibiotic cocktail consisted of vancomycin (0.5 mg/mL), ampicillin (1 mg/mL), metronidazole (1 mg/mL), and neomycin sulfate (1 mg/mL) (Shanghai Macklin Biochemical Co., Ltd.).

Each bacterial strain was cultured separately in lysogeny broth (LB) at 37 ℃ with shaking at 200 rpm for 48 h. Bacterial cells were harvested by centrifugation, washed with sterile PBS, and resuspended in PBS before oral administration. Following antibiotic treatment, mice were gavaged with 0.2 mL of the corresponding bacterial suspension. To evaluate whether the effect of *P. fortuita* was mediated by urease-dependent ammonia production, mice receiving *P. fortuita* were treated with FFA, a bacterial urease inhibitor, at 6 mg/kg by intraperitoneal injection. Control mice received vehicle treatment under the same conditions. Fecal ammonia levels were measured after intervention, and cognitive performance was assessed using the Y-maze test, novel object recognition test, and Morris water maze test.

In vitro co-culture of _P. fortuita_ with FFA

To validate whether FFA inhibited *P. fortuita*-derived urease-mediated ammonia production without markedly affecting bacterial growth, *P. fortuita* was cultured in urea-containing medium with or without FFA. The urea-containing medium provided urea as the urease substrate, and the same medium without bacteria served as the blank control. *P. fortuita* was inoculated into the medium and incubated at 37 ℃ with shaking. Bacterial growth was monitored by measuring OD_{600} at the indicated time points. After incubation, cultures were centrifuged to collect the supernatants. Ammonia levels and urease activity in the culture supernatants were measured using commercial assay kits according to the manufacturers' instructions. This assay was used to determine whether FFA reduced *P. fortuita*-associated urease activity and ammonia production independently of bacterial growth inhibition.

Fecal qPCR analysis of _P. fortuita_ and _P. fortuita_-derived urease abundance

To evaluate the effects of FFA on the fecal *P. fortuita*-associated transcriptional signal and urease-related gene expression, fecal samples were collected from mice treated with *P. fortuita* alone or *P. fortuita* plus FFA. Total fecal RNA was extracted using a commercial RNA extraction kit according to the manufacturer's instructions. RNA concentration and purity were assessed, and equal amounts of RNA were reverse-transcribed into complementary DNA using a commercial reverse-

transcription kit.

Quantitative real-time PCR was performed using *P. fortuita*-specific 16S rRNA primers and *P. fortuita ureC*-specific primers. Universal bacterial 16S rRNA was used as the reference for normalization. The primer sequences were as follows:

P. fortuita-F: 5‘-TAGGAAGGAACACCAGTGGCGAAG-3’
P. fortuita-R: 5‘-GTTGACATCGTTTACGGCGTGGAC-3’
P. fortuita ureC-F: 5‘-GTGGCGATCCATACCGACACC-3’
P. fortuita ureC-R: 5‘-GAAGGTGTGGATGGTCCGGTC-3’
universal bacterial 16S-F: 5‘-GTAGTCCACGCCGTAAACGA-3’
universal bacterial 16S-R: 5 ‘-CCGAAGGCACCAATCTATCTC-3’

Relative transcript levels were calculated using the $2^{-\Delta\Delta Ct}$ method, with ΔCt defined as the difference between the Ct value of the target gene and that of universal bacterial 16S rRNA gene. The mean ΔCt value of the *P. fortuita*-treated group was used as the calibrator.

RNA-seq and transcriptomic analysis

Total RNA was extracted from colon and brain using TRIzol reagent (Invitrogen), followed by DNase I treatment (TaKaRa) to remove residual genomic DNA. RNA integrity and concentration were assessed using an Agilent 2100 Bioanalyzer in combination with a NanoDrop ND-2000 spectrophotometer. For library preparation, 1 μg of DNase-treated RNA was used to construct sequencing libraries with the Illumina TruSeq RNA Sample Preparation Kit. Polyadenylated mRNA was enriched using oligo(dT) magnetic beads, fragmented, and reverse-transcribed to generate cDNA. The resulting cDNA fragments were subjected to end repair, A-tailing, and ligation to indexed sequencing adapters, followed by size selection (200-300 bp) using 2% Low Range Ultra Agarose. Libraries were amplified by 15 cycles of PCR using Phusion DNA Polymerase (NEB) and quantified prior to sequencing. Paired-end sequencing was performed by BIOZERON Co., Ltd. Raw sequencing reads were quality-filtered using Fastp and aligned to the mouse reference genome (GRCm39) with Hisat2 [15]. Differential gene expression analysis was carried out using DESeq2 [16]. Gene set enrichment analysis (GSEA) was conducted with the clusterProfiler R package [17], and pathway annotation was performed based on the KEGG database.

Cell lines and culture conditions

HEK293FT cells were maintained in our in-house laboratory. NIH3T3 mouse embryonic fibroblasts (GL0021) were obtained from Geneline Bioscience (Beijing, China). Caco-2 human intestinal epithelial cells (CL-0050) were purchased from Procell Life Science & Technology Co., Ltd. (Wuhan, China). C8-D1A mouse cerebellar astrocytes (CL-0506) were purchased as C8-D1A (STR) cells from Procell Life Science & Technology Co., Ltd. (Wuhan, China). IMCCs (FH-Y064) were purchased from FuHeng Biology (Shanghai, China).

HEK293FT, NIH3T3, Caco-2, and C8-D1A cells were cultured in Dulbecco’s Modified Eagle Medium (DMEM) supplemented with 10% serum and 1% penicillin/streptomycin. Specifically, HEK293FT and NIH3T3 cells were maintained in DMEM containing 10% bovine calf serum, whereas Caco-2 and C8-D1A cells were maintained in DMEM containing 10% fetal bovine serum. IMCCs were cultured in the specialized complete medium recommended by the supplier. All cells

were maintained at 37 ℃ in a humidified incubator containing 5% CO_2.

Transwell epithelial cell-astrocyte co-culture assay

To evaluate whether epithelial SMAD7 could influence JAK2 signaling in brain-related cells, a Transwell co-culture system was established using IMCCs and C8-D1A mouse astrocytes. IMCCs were used as the epithelial compartment, whereas C8-D1A cells were used as the astrocytic compartment. The Transwell system allowed soluble factors released from epithelial cells to diffuse into the lower chamber without direct cell-cell contact.

Briefly, IMCCs were first seeded in 12-well plates and transfected with the SMAD7 overexpression plasmid or the corresponding empty vector control. Twenty-four hours after transfection, IMCCs were gently detached, collected, and reseeded into the upper chamber of Transwell inserts. C8-D1A cells were seeded in the lower wells and cultured in DMEM supplemented with 10% fetal bovine serum and 1% penicillin/streptomycin. The Transwell inserts containing transfected IMCCs were then placed above the C8-D1A cells to initiate epithelial cell-astrocyte co-culture. After co-culture for 48 h, C8-D1A cells in the lower chamber were collected for protein extraction, and JAK2 protein levels were assessed by western blotting.

Western Blot Analysis

Cells were washed with PBS and lysed on ice for 30 min in RIPA buffer (Beyotime) supplemented with protease inhibitors. Lysates were centrifuged at 12,000 × g for 10 min at 4 ℃, and the supernatants were collected for protein analysis. Protein samples were combined with 5× loading buffer, denatured at 95 ℃ for 5 min, and separated on 10% Tris-glycine SDS-PAGE gels, followed by transfer onto PVDF membranes. Membranes were blocked with 5% nonfat milk in TBST for 1 h at room temperature and then incubated overnight at 4 ℃ with primary antibodies against (SMAD7, mouse, 1:500, bsm-33869M, Bioss; JAK2, rabbit, 1:500, bs-0908R, Bioss; Flag, rabbit, 1:20000, 20543-1-AP, Proteintech). After three washes with TBST, membranes were incubated with HRP-conjugated secondary antibodies (goat anti-rabbit or goat anti-mouse IgG, 1:5000; Bioss) for 1 h at room temperature. Protein bands were visualized using enhanced chemiluminescence (Ultra ECL, Biosharp) and quantified with ImageJ software. GAPDH (mouse, 1:50000, 60004-1-Ig, Proteintech) was used as the loading control.

Cellular Immunofluorescence Staining

To investigate the subcellular localization of SMAD7 and JAK2 following ammonia treatment, cells were subjected to immunofluorescence staining. Cells cultured in 24-well plates were fixed with 4% paraformaldehyde for 15 min, then permeabilized and blocked with a buffer containing 5% BSA, 10% normal goat serum, and 0.3% Triton X-100 in PBS for 1 h at room temperature. Cells were incubated overnight at 4 ℃ with primary antibodies against (SMAD7, rabbit, 1:1000, 25840-1-AP, Proteintech; JAK2, rabbit, 1:1000, 3230T, Cell signaling TECHNOLOGY; Flag, rabbit, 1:1000, 20543-1-AP, Proteintech; HA, mouse, 1:1000,66006-2-Ig, Proteintech). After washing with PBS, cells were incubated for 1 h at room temperature with Goat Anti-Mouse IgG H&L, BF488 conjugated (1:5000, bs-0296G-BF488, Bioss) , Goat Anti-Rabbit IgG H&L, Cy3 conjugated (1:5000, bs-0295G-Cy3, Bioss) and counterstained with DAPI (C0065, Solarbio). Coverslips were mounted using antifade mounting medium, and fluorescence images were captured using an inverted fluorescence microscope. Quantification of fluorescence intensity was performed using

ImageJ software.

Plasmid transfection

Cells used for plasmid transfection were seeded into culture plates at an appropriate density according to their growth characteristics and transfected when cell confluency reached approximately 70-80%. Culture medium was replaced with fresh complete medium 1 h before transfection. Transfections were performed using Vigofect transfection reagent. For a 12-well plate, 50 μL of 150 mM NaCl containing 2.5 μg plasmid DNA (SMAD7:JAK2 = 1:1) and 50 μL of 150 mM NaCl containing 1 μL Vigofect were prepared separately for each well, gently mixed, and incubated for 5 min. The DNA and Vigofect solutions were then combined, incubated for an additional 15 min, and added dropwise to the cells. Cells were returned to the incubator and cultured at 37 ℃ with 5% CO_2. Samples were collected 24 h after transfection.

AAV preparation and rectal enema-mediated colonic SMAD7 overexpression

To restore colonic SMAD7 expression in MCI mice, an adeno-associated virus expressing mouse Smad7 was constructed and packaged by General Biol (Anhui) Co., Ltd. (Anhui, China). The full-length mouse Smad7 sequence with a 3×Flag tag was inserted into the AAV expression vector VA275-AAV-Villin-MCS-T2A-ZsGreen to generate AAV-SMAD7. The Villin promoter was used to drive intestinal epithelial-enriched transgene expression. A corresponding control AAV vector with the same backbone was used as the negative control. The viral serotype was AAV9. Recombinant AAV particles were produced in 293T cells using a standard triple-plasmid AAV packaging system, including the transgene-carrying AAV vector plasmid, the AAV9 packaging plasmid, and the helper plasmid. Viral particles were harvested, purified, concentrated, and subjected to quality control by the manufacturer. Viral genome titer was determined by quantitative PCR. The final titer of AAV-SMAD7 was 4.87×10^{12} viral genomes/mL. Sterility testing and mycoplasma testing were negative. Viral aliquots were stored at -80 ℃ and thawed on ice immediately before use.

After establishment of the 5-FU-induced MCI-like model, mice were treated with AAV-SMAD7 or control AAV by rectal enema. Briefly, mice were gently anesthetized and placed in a head-down position. A flexible sterile catheter was lubricated and inserted gently into the rectum to deliver the viral suspension into the distal colon. Each mouse received approximately 1×10^{12} viral genomes of AAV-SMAD7 or control AAV in a volume of approximately 200 μL. After administration, mice were maintained in a head-down position for several minutes to reduce leakage and promote retention of the viral suspension in the colonic lumen. Control mice received the same viral dose and volume of control AAV vector under identical conditions. After AAV intervention, behavioral performance was evaluated using the Y-maze test, novel object recognition test, and Morris water maze test. At the end of the experiment, colonic tissues were collected to verify SMAD7 overexpression by western blotting, and brain tissues were collected to assess JAK2 protein levels.

***L. mucosae* intervention and ammonia-lowering validation**

L. mucosae was obtained from our in-house bacterial library and used as an intestinal ammonia-lowering intervention strain. To determine whether the effect of *L. mucosae* required viable bacterial metabolism and was not simply caused by bacterial structural components or nonspecific Lactobacillus supplementation, heat-killed *L. mucosae* and live *L. fermentum* were included as

additional controls.

Heat-killed *L. mucosae* was prepared from live *L. mucosae* cultures. Briefly, *L. mucosae* was cultured, harvested by centrifugation, washed with sterile PBS, and resuspended to the same bacterial density as the live bacterial suspension. The suspension was then heated at 80 ℃ for 30 min to inactivate the bacteria. The heat-killed bacterial suspension was cooled to room temperature before use.

For the in vitro ammonia-lowering assay, live *L. mucosae*, heat-killed *L. mucosae*, and live *L. fermentum* were pre-cultured, washed with sterile PBS, and resuspended to comparable bacterial densities. The bacterial suspensions were added to medium containing 5 mM NH_4Cl and glucose and incubated at 37 ℃ for 24 h. Medium without bacteria served as the blank control. After incubation, cultures were centrifuged, and supernatants were collected for NH_4^+ measurement using the Ammonia Content Assay Kit according to the manufacturer's instructions.

For the in vivo intervention experiment, mice were first treated with the 7-day antibiotic cocktail described above. After antibiotic treatment, mice were orally gavaged with 0.2 mL of live *L. mucosae*, heat-killed *L. mucosae*, or live *L. fermentum* suspension under the same experimental conditions. Fecal ammonia levels were measured after intervention, and cognitive performance was evaluated using the Y-maze test, novel object recognition test, and Morris water maze test.

Statistical analysis

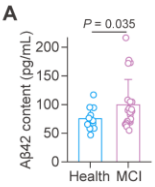
Animals were randomly assigned to experimental groups, and data collection was performed in a randomized manner. Investigators were blinded to group allocation during both the collection and analysis of data. Sample sizes were chosen based on prior experience and previous studies conducted in our laboratory. Statistical analyses were conducted using R software, with specific packages indicated in the corresponding Methods sections. Statistical significance was assessed using a two-tailed Student's t-test for comparisons between two groups or one-way ANOVA followed by Fisher's LSD post hoc test for comparisons involving three or more groups. Each data point corresponds to an independent biological replicate, and all experiments were performed with a minimum of three independent biological replicates.

SI Figure legends

Characteristics	Health (n = 20)	MCI (n = 28)	P-value
Age in years, y (SD)	68.55 (8.00)	73.00 (9.11)	0.08
Females, n (%)	7 (35.0 %)	18 (64.3 %)	0.078
MMSE score, mean (SD)	29.70 (0.92)	9.43 (7.74)	< 0.001
MoCA score, mean (SD)	29.25 (1.12)	8.50 (7.30)	< 0.001
Diabetes, n (%)	5 (25.0 %)	8 (28.6 %)	1.0
Hypertension, n (%)	6 (30.0 %)	10 (35.7 %)	0.763
Coronary heart disease, n (%)	1 (5.0 %)	2 (7.1 %)	1.0
Dyslipidemia, n (%)	4 (20.0 %)	5 (17.9 %)	1.0

Supplementary Figure 1 Baseline demographic and clinical characteristics of the independent clinical cohort. Data are presented as mean (SD) for continuous variables and n (%) for categorical variables. Continuous variables were compared using an independent two-sample Student's t-test, and categorical variables were compared using Fisher's exact test. MMSE, Mini-Mental State Examination; MoCA, Montreal Cognitive Assessment.

A



B

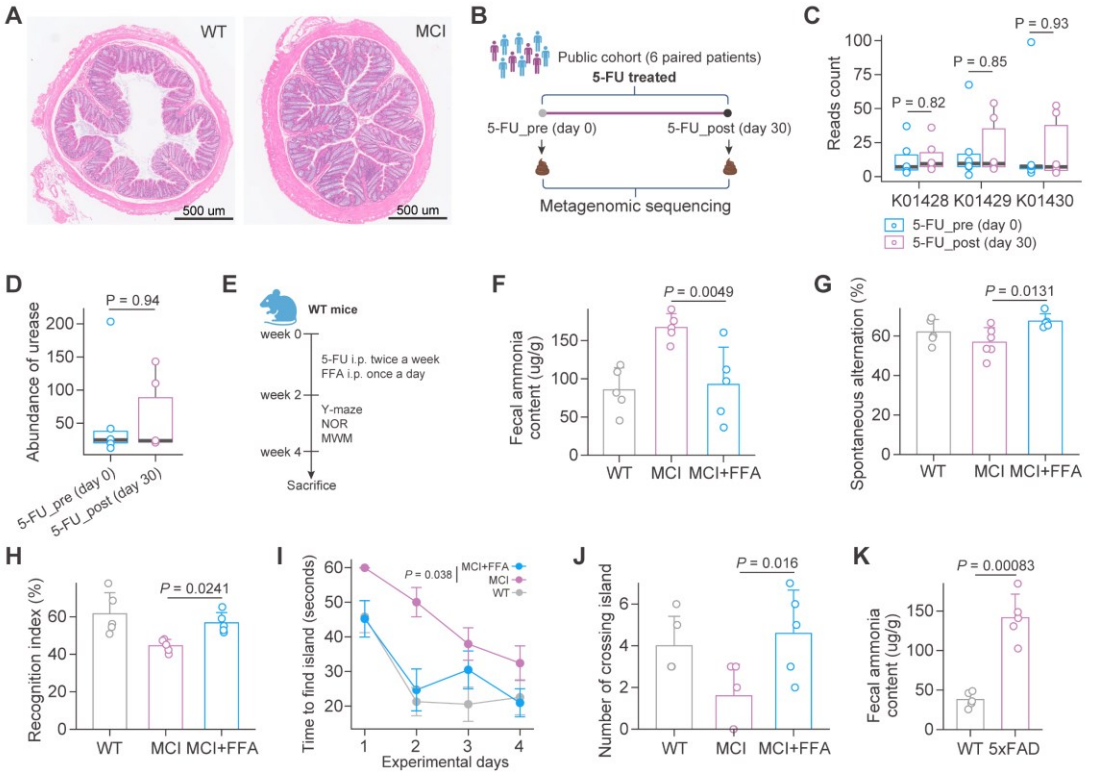
APOE genotyping	Health (n = 12)	MCI (n = 21)
ε3 / ε3	7 (58.3 %)	7 (33.3 %)
ε3 / ε4	2 (16.7 %)	9 (42.9 %)
ε4 / ε4	0 (0 %)	2 (9.5 %)
ε2 / ε3	3 (25 %)	2 (9.5 %)
ε2 / ε4	0 (0 %)	1 (4.8 %)

C

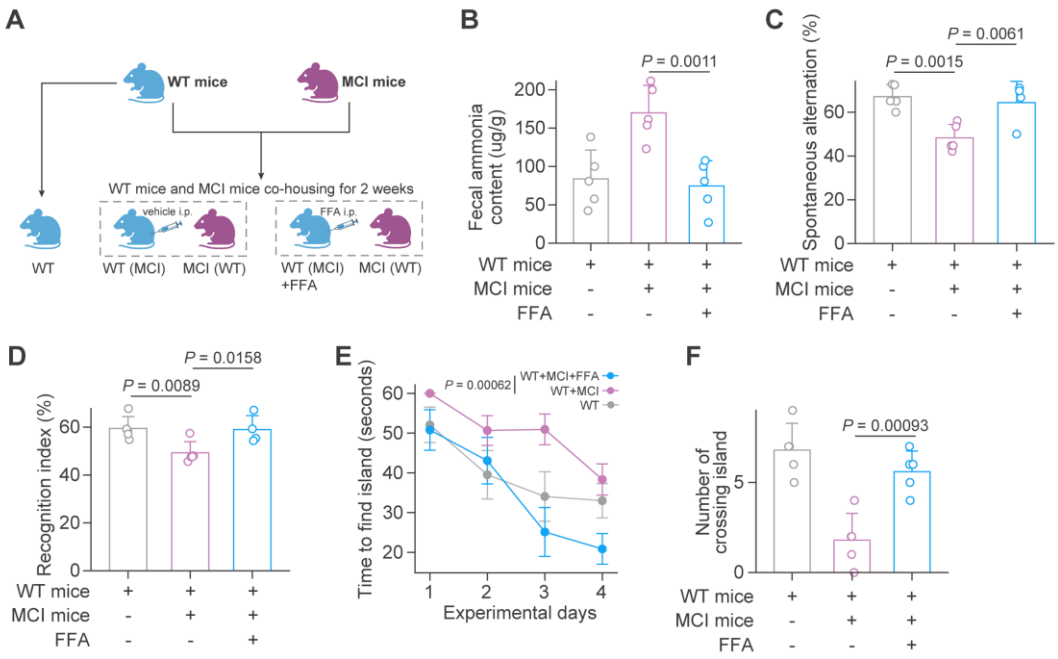
Indicator	Health (n = 12)	MCI (n = 21)	P-value
ε4 carrier frequency	2 / 12 (16.7 %)	12 / 21 (57.1 %)	0.033
ε4 allele frequency	2 / 24 (8.3 %)	14 / 42 (33.3 %)	0.035

(1) ε4 carrier frequency was defined as the proportion of individuals carrying at least one APOE ε4 allele.
(2) ε4 allele frequency was defined as the proportion of ε4 alleles among all APOE alleles.
(3) Differences between groups were assessed using Fisher's exact test.

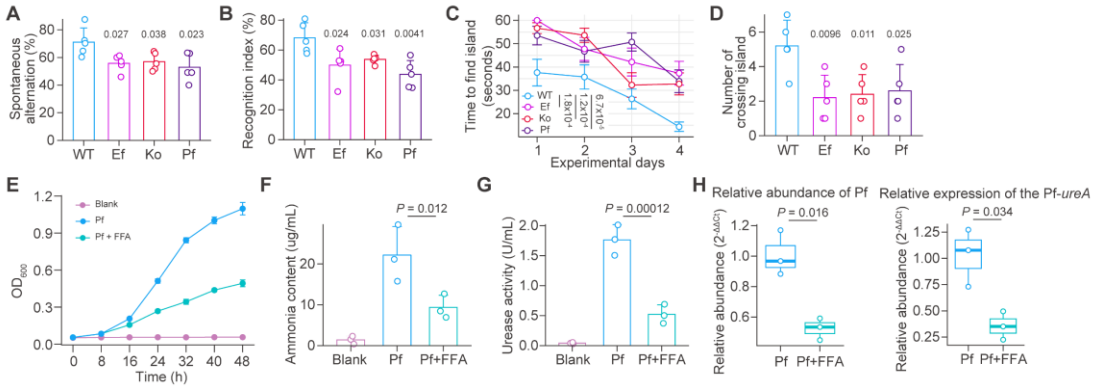
Supplementary Figure 2 AD-related biomarker and APOE ε4 risk features in the independent clinical cohort. (**A**) Aβ42 concentrations in available samples from healthy controls and participants with MCI. Data are presented as mean ± s.d. Statistical significance was assessed using a two-tailed Student's t-test. (**B**) Distribution of APOE genotypes among genotyped healthy controls and participants with MCI. (**C**) Comparison of APOE ε4 carrier frequency and ε4 allele frequency between healthy controls and participants with MCI. APOE ε4 carrier frequency was defined as the proportion of individuals carrying at least one ε4 allele, whereas APOE ε4 allele frequency was defined as the proportion of ε4 alleles among all APOE alleles. Differences between groups were assessed using Fisher's exact test.



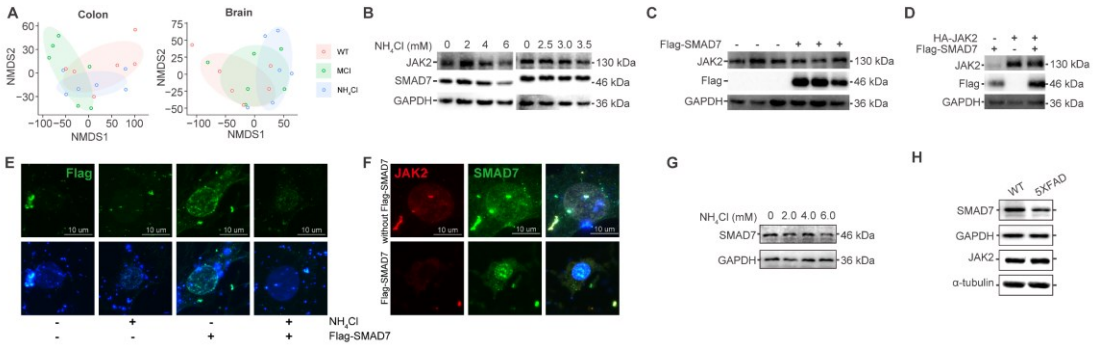
Supplementary Figure 3 Validation of the 5-FU-induced MCI-like model, FFA-mediated rescue, and intestinal ammonia elevation in 5xFAD mice. (**A**) Representative hematoxylin and eosin (H&E)-stained intestinal sections from WT and 5-FU-induced MCI-like mice. (**B**) Schematic representation of the paired public fecal metagenomic cohort. Fecal samples from six patients were collected before 5-FU treatment on day 0 and after treatment on day 30 for metagenomic sequencing. (**C**) Paired comparison of the abundance of the urease-associated genes K01428, K01429, and K01430 before and after 5-FU treatment. (**D**) Paired comparison of predicted total urease abundance before and after 5-FU treatment. (**E**) Experimental timeline for FFA intervention in the 5-FU-induced MCI-like mouse model. Mice received 5-FU by intraperitoneal injection twice weekly and FFA by intraperitoneal injection once daily, followed by behavioral testing using the Y-maze, novel object recognition test, and Morris water maze. (**F**) Fecal ammonia concentrations in WT, untreated MCI-like, and FFA-treated MCI-like mice. (**G**) Spontaneous alternation percentages in the Y-maze test. (**H**) Recognition index in the novel object recognition test. (**I**) Escape latency during the acquisition phase of the Morris water maze test. (**J**) Number of crossings over the previous platform location during the probe trial. (**K**) Fecal ammonia concentrations in WT and 5xFAD mice at an early disease stage.



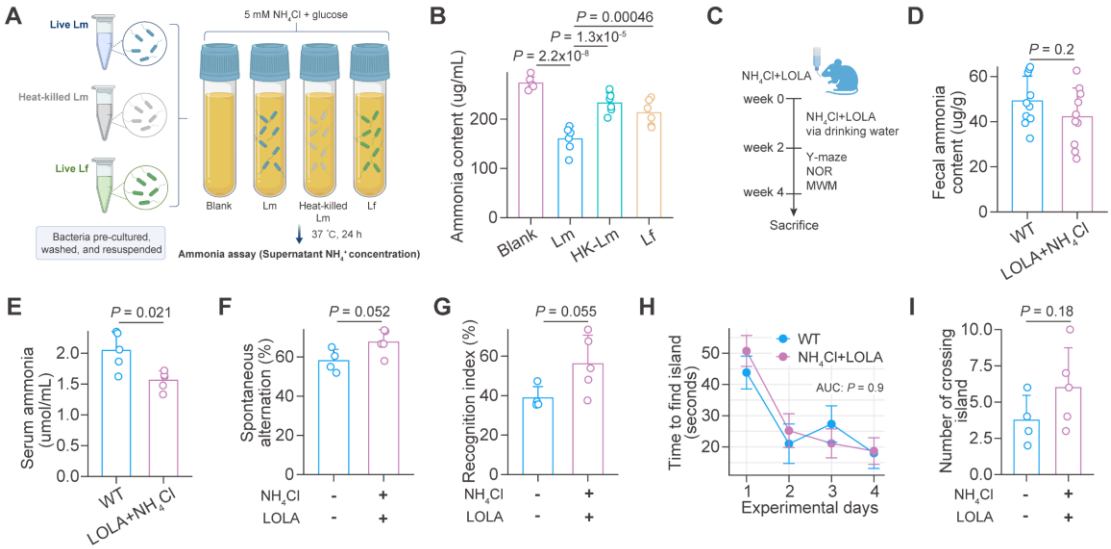
Supplementary Figure 4 FFA attenuates the ammonia-related cognitive phenotype transmitted to WT mice by cohousing with MCI-like mice. (**A**) Schematic illustration of the cohousing and FFA intervention experiment. WT and 5-FU-induced MCI-like mice were cohoused for 2 weeks. Cohoused mice received either vehicle or FFA by intraperitoneal injection. Separately housed WT mice served as controls. WT (MCI) denotes WT mice cohoused with MCI-like mice, whereas MCI (WT) denotes MCI-like mice cohoused with WT mice. Subsequent analyses focused on the WT recipient mice. (**B**) Fecal ammonia concentrations in separately housed WT mice, WT mice cohoused with MCI-like mice, and FFA-treated WT mice cohoused with MCI-like mice. (**C**) Spontaneous alternation percentages in the Y-maze test. (**D**) Recognition index in the novel object recognition test. (**E**) Escape latency during the acquisition phase of the Morris water maze test. (**F**) Number of crossings over the previous platform location during the probe trial.



Supplementary Figure 5 Comparative behavioral effects of urease-positive bacterial isolates and validation of FFA effects on *P. fortuita*-associated ammonia production. (**A**) Spontaneous alternation percentages in the Y-maze test in WT mice and mice administered *Enterococcus faecium* (Ef), *Klebsiella oxytoca* (Ko), or *Pseudomonas fortuita* (Pf). (**B**) Recognition index in the novel object recognition test. (**C**) Escape latency during the acquisition phase of the Morris water maze test. (**D**) Number of crossings over the previous platform location during the probe trial. (**E**) Growth curves of *P. fortuita* cultured in the absence or presence of FFA, with sterile medium serving as the blank control. Bacterial growth was monitored by measuring OD_{600} at the indicated time points. (**F**) Ammonia concentrations in culture supernatants from the blank, Pf, and Pf+FFA groups. (**G**) Urease activity in culture supernatants from the blank, Pf, and Pf+FFA groups. (**H**) Fecal RT-qPCR analysis of the *P. fortuita*-specific 16S rRNA gene and the *P. fortuita*-derived ureA transcript level in mice administered Pf alone or Pf plus FFA. Universal bacterial 16S rRNA was used for normalization, and relative transcript levels were calculated using the $2^{-\Delta\Delta Ct}$ method.



Supplementary Figure 6 Transcriptomic and cellular validation of ammonia-associated SMAD7-JAK2 signaling. (**A**) Non-metric multidimensional scaling (NMDS) analysis of brain and colonic transcriptomic profiles from WT, 5-FU-induced MCI-like, and NH_4Cl-treated mice. (**B**) Immunoblot analysis of JAK2 and SMAD7 protein expression in HEK293FT cells exposed to the indicated concentrations of NH_4Cl. (**C**) Immunoblot analysis of endogenous JAK2 expression in HEK293FT cells transfected with the Flag-SMAD7 expression plasmid or the corresponding empty-vector control. Flag immunoblotting was used to verify SMAD7 overexpression, and GAPDH served as the loading control. (**D**) Immunoblot analysis of JAK2 protein expression in HEK293FT cells transfected with HA-JAK2 alone or co-transfected with HA-JAK2 and Flag-SMAD7. Flag immunoblotting was used to confirm SMAD7 overexpression, and GAPDH served as the loading control. (**E**) Representative immunofluorescence images showing Flag-SMAD7 signals in cells with or without NH_4Cl treatment. Cells were transfected with the Flag-SMAD7 plasmid or the corresponding empty vector, as indicated. Nuclei were counterstained with DAPI. Scale bars, 10 μm. (**F**) Representative immunofluorescence images showing JAK2 (red) and SMAD7 (green) in cells transfected with Flag-SMAD7 or the corresponding empty-vector control. Nuclei were counterstained with DAPI, and merged images are shown. Scale bars, 10 μm. (**G**) Immunoblot analysis of SMAD7 expression in IMCCs exposed to the indicated concentrations of NH_4Cl. (**H**) Representative immunoblot analysis of colonic SMAD7 and brain JAK2 protein levels in WT and 5xFAD mice.



Supplementary Figure 7 In vitro ammonia-lowering capacity of *Limosilactobacillus mucosae* and effects of L-ornithine L-aspartate in NH_4Cl-treated mice. (**A**) Schematic illustration of the in vitro ammonia-lowering assay. Live *Limosilactobacillus mucosae* (Lm), heat-killed *L. mucosae* (HK-Lm), and live *Limosilactobacillus fermentum* (Lf) were pre-cultured, washed, resuspended, and incubated for 24 h at 37 °C in medium containing 5 mM NH_4Cl and glucose. Medium without bacteria served as the blank control. Ammonia concentrations were subsequently measured in the culture supernatants. (**B**) Ammonia concentrations in culture supernatants from the blank, live Lm, HK-Lm, and live Lf groups. (**C**) Experimental timeline for combined NH_4Cl and L-ornithine L-aspartate (LOLA) administration in mice, followed by behavioral testing using the Y-maze, novel object recognition test, and Morris water maze. (**D**) Fecal ammonia concentrations in WT and NH_4Cl +LOLA-treated mice. (**E**) Serum ammonia concentrations in WT and NH_4Cl +LOLA-treated mice. (**F**) Spontaneous alternation percentages in the Y-maze test. (**G**) Recognition index in the novel object recognition test. (**H**) Escape latency during the acquisition phase of the Morris water maze test. The area under the curve was compared between groups. (**I**) Number of crossings over the previous platform location during the probe trial.

A

Components	Food composition (some typical examples)
Staple foods	White rice, brown rice, sweet potato rice, pumpkin rice, noodles, porridge
Vegetables	Spinach, Chinese cabbage, lettuce, leaf lettuce, pumpkin, bitter melon, potato, carrot
Animal-protein sources	Pork, chicken, duck, fish fillets, shrimp, eggs, sliced meat soup, pork rib/bone soup
Soy products / plant-based protein	Soy milk, tofu, green beans/cowpeas, potatoes, bean sprouts
Soups	Sliced meat soup, pork rib/bone soup, chicken soup, vegetable soup, coix seed soup

(1) Standardized meals provided by the same elderly care facility.
(2) Standardized meals were vegetable-dominant, lightly seasoned, with animal protein as a supplement.

B

Nutrient component	Content
Crude protein	>18 %
Crude fat	>4 %
Crude fiber	<5 %
Crude ash	<8 %
Moisture	<10 %
Calcium	1.0-1.8 %
Phosphorus	0.6-1.2 %

Supplementary Figure 8 Dietary characteristics of the clinical cohort and nutrient composition of the mouse chow. (**A**) Representative food categories and typical meal components provided to participants in the independent clinical cohort. All participants received standardized meals prepared by the same elderly care facility. The meals were generally vegetable-dominant and lightly seasoned, with animal-protein sources provided as supplementary components. (**B**) Nutrient composition of the standard laboratory chow provided to all mice during the experiments.

SI references lists

1. Jia, L., et al., Metagenomic analysis characterizes stage-specific gut microbiota in Alzheimer's disease. *Mol Psychiatry*, 2025. **30**(9): 3951-3962.

2. Wan, L., et al., Mutational Pattern Induced by 5-Fluorouracil and Oxaliplatin in the Gut Microbiome. *Front Microbiol*, 2022. **13**: 841458.

3. Gallego-Duran, R., et al., Ammonia-induced stress response in liver disease progression and hepatic encephalopathy. *Nat Rev Gastroenterol Hepatol*, 2024. **21**(11): 774-791.

4. Chen, S., Y. Zhou, Y. Chen, and J. Gu, fastp: an ultra-fast all-in-one FASTQ preprocessor. *Bioinformatics*, 2018. **34**(17): i884-i890.

5. Langdon, W.B., Performance of genetic programming optimised Bowtie2 on genome comparison and analytic testing (GCAT) benchmarks. *BioData Min*, 2015. **8**(1): 1.

6. Li, D., et al., MEGAHIT: an ultra-fast single-node solution for large and complex metagenomics assembly via succinct de Bruijn graph. *Bioinformatics*, 2015. **31**(10): 1674-6.

7. Xu, H., et al., FastUniq: a fast de novo duplicates removal tool for paired short reads. *PLoS One*, 2012. **7**(12): e52249.

8. Lu, J., F.P. Breitwieser, P. Thielen, and S.L. Salzberg, Bracken: estimating species abundance in metagenomics data. *PeerJ Comput Sci*, 2017. **3**.

9. Wood, D.E., J. Lu, and B. Langmead, Improved metagenomic analysis with Kraken 2. *Genome Biol*, 2019. **20**(1): 257.

10. Fu, L., et al., CD-HIT: accelerated for clustering the next-generation sequencing data. *Bioinformatics*, 2012. **28**(23): 3150-2.

11. Huerta-Cepas, J., et al., Fast Genome-Wide Functional Annotation through Orthology Assignment by eggNOG-Mapper. *Mol Biol Evol*, 2017. **34**(8): 2115-2122.

12. Hyatt, D., et al., Prodigal: prokaryotic gene recognition and translation initiation site identification. *BMC Bioinformatics*, 2010. **11**: 119.

13. Patro, R., et al., Salmon provides fast and bias-aware quantification of transcript expression. *Nat Methods*, 2017. **14**(4): 417-419.

14. Chen, H., et al., Gut microbial ammonia enhances colonic acetylcholine levels to regulate intestinal motility. *Nat Microbiol*, 2026. **11**(4): 907-919.

15. Kim, D., et al., Graph-based genome alignment and genotyping with HISAT2 and HISAT-genotype. *Nat Biotechnol*, 2019. **37**(8): 907-915.

16. Love, M.I., W. Huber, and S. Anders, Moderated estimation of fold change and dispersion for RNA-seq data with DESeq2. *Genome Biol*, 2014. **15**(12): 550.

17. Yu, G., L.G. Wang, Y. Han, and Q.Y. He, clusterProfiler: an R package for comparing biological themes among gene clusters. *OMICS*, 2012. **16**(5): 284-7.